Crystal Structures of Two Cobalt Complexes with Tetrahedrally Distorted Trigonal Bipyramidal Co-ordination and Semiempirical Molecular Orbital Study of the Distortion

By **Massimo Di Vaira**, Istituto di Chimica Generale ed Inorganica dell'Università di Firenze, Laboratorio per lo Studio della Stereochimica ed Energetica dei Composti di Coordinazione del C.N.R., 41 Via J. Nardi, Firenze, Italy

The crystal and molecular structures of two high-spin cobalt(II) complexes with the ligand tris(2-diphenylphosphinoethyl)amine (np) have been determined by *X*-ray diffraction. Crystals of [Co(np)Br][PF_6],EtOH, (I), are triclinic, space group $P\bar{1}$, with a = 10.51, b = 18.10, c = 13.09 Å, α = 110.78°, β = 94.95°, γ = 98.68°, Z = 2. Crystals of [Co(np)I][BPh_4], MePh, (II), are triclinic, space group $P\bar{1}$, with a = 16.555(1), b = 18.780(1), c = 10.168 (1) Å, α = 84.83(1)°, β = 88.14(1)°, γ = 95.48(1)°, Z = 2. For complex (I) 2 119 reflections were collected by photographic methods, and 4510 by counter methods for (II). The structures were solved by heavy-atom techniques and final R values are 0.098 (I) and 0.115 (II). The co-ordination is trigonal bipyramidal with large tetrahedral distortion in both complexes and is similar to that previously found in the corresponding chloro-derivative. Complex (II) is the only high-spin iodo-derivative in this series. The unusually large temperature factor of the halogen atom in both structures is attributed to a pseudo-Jahn–Teller effect. Semiempirical MO calculations have been performed on simplified models, reproducing complexes of this series and of related series, in order to understand which factors determine the geometry of co-ordination in this series of complexes.

THE spin state of the metal atom in five-co-ordinate Co^{II} and Ni^{II} complexes is determined to some extent by the nature of the donor set.[1] A connection between the spin state and the geometry of co-ordination is also found for certain donor sets.[2]

Previous investigations have shown that the spin multiplicity and the geometry of five-co-ordination about cobalt, in the series of complexes[3] of formula [Co(np)X]Y, where np is the tripod ligand tris(2-diphenylphosphinoethyl)amine, $(Ph_2PCH_2CH_2)_3N$, X = Cl, Br, I, or NCS, and Y = X, BF_4, PF_6, or BPh_4, depend on the nature of the substituents X or Y. Complexes are high-spin when X = Cl or Br, irrespective of the nature of the counter-ion.[3] Determination of the structure of [Co(np)Cl][PF_6] had revealed tetrahedrally-distorted trigonal bipyramidal co-ordination.[4] Complexes are low-spin when X = I or NCS, except for the complex [Co(np)I][BPh_4], which has a quadruplet ground-state in the solid. In the structure of low-spin [Co(np)I]I distorted square-pyramidal co-ordination has been found.[5] All the nickel complexes of this

[1] L. Sacconi, *J. Chem. Soc.* (*A*), 1970, 248.

[2] (*a*) L. Sacconi, *Co-ordination Chem. Rev.*, 1972, **8**, 351; (*b*) R. Morassi, I. Bertini, and L. Sacconi, *ibid.*, 1973, **11**, 343.

[3] L. Sacconi and I. Bertini, *J. Amer. Chem. Soc.*, 1968, **90**, 5443.

[4] M. Di Vaira and A. Bianchi Orlandini, *Inorg. Chem.*, 1973, **12**, 1292.

[5] C. Mealli, P. L. Orioli, and L. Sacconi, *J. Chem. Soc.* (*A*), 1971, 2691.

series are low-spin [3] and trigonal bipyramidal co-ordination has been found for [Ni(np)I]I (ref. 6) and [Ni(np)Cl][PF_6].[7]

The study of the structures of the complexes [Co(np)Br][PF_6] and [Co(np)I][BPh_4] by *X*-ray was undertaken in order to understand whether the intermediate 4 + 1 co-ordination found for the chloro-derivative [4] may be assigned to all high-spin cobalt complexes of this series. It was also expected that comparisons might help to elucidate all possible aspects of this unusual co-ordination. Special interest in the iodo-derivative was due to its exceptional high-spin state; possible comparisons were also expected with the low-spin complex of ref. 5.

The experimental geometries, somewhat idealized, have been referred to, in performing a set of semi-empirical MO calculations of the extended-Hückel (EH) self-consistent charge and configuration (SCCC) type. These were undertaken to obtain some understanding of the origin of the tetrahedral distortion in this series of complexes.

EXPERIMENTAL

Crystal Data.—(*a*) [Co(np)Br][PF_6],EtOH, (I), $C_{44}H_{48}BrCoF_6NOP_4$, $M = 982.14$, Triclinic, $a = 10.51$, $b = 18.10$, $c = 13.09$ Å, $\alpha = 110.78°$, $\beta = 94.95°$, $\gamma = 98.68°$, $U = 2\,274.8$ Å^3, $D_c = 1.42$ (by flotation), $Z = 2$, $D_c = 1.43$, $F(000) = 1\,076$. Space group $P\bar{1}$. Fe-K_α radiation, $\lambda = 1.9373$ Å; μ(Fe-K_α) = 69.0 cm^{-1}. (*b*) [Co(np)I][BPh_4],C_7H_8, (II), $C_{73}H_{70}BCoINP_3$, $M = 1\,250.95$, Triclinic, $a = 16.555(1)$, $b = 18.780(1)$, $c = 10.168(1)$ Å, $\alpha = 84.83(1)°$, $\beta = 88.14(1)°$, $\gamma = 95.48(1)°$, $U = 3\,133.1$ Å^3, $D_m = 1.35$ (by flotation), $Z = 2$, $D_c = 1.32$, $F(000) = 1\,290$, Space group $P\bar{1}$. Mo-K_α radiation, $\lambda = 0.70926$ Å; μ (Mo-K_α) = 9.69 cm^{-1}.

Data Collection.—(*a*) Crystals of (I) were prepared as described in ref. 3 and recrystallized from ethanol. Cell constants were obtained from 0*kl* and *h*0*l* Weissenberg photographs. Owing to the bad quality of the crystals it was impossible to collect Weissenberg data along a third direction, for an accurate estimate of the errors on lattice constants; errors should be <0.5% of parameter values reported.

The reciprocal lattice levels 0—6*kl* were collected on a Nonius integrating Weissenberg camera with manganese-filtered Fe-K_α radiation, by the multiple-film equi-inclination technique. The intensities of 2 119 reflections were measured on a Nonius microdensitometer. The various levels were put on a common scale by means of two Weissenberg photographs, which contained 30° samples from each level, one sample being common to the two photographs. The two parts into which each level was split during data collection, because of the triclinic space group, were initially scaled with the use of a few common reflections. The crystal used for data collection had prismatic elongated form, along [100], with dimensions *ca.* 0.60 × 0.18 × 0.10 mm. No correction for absorption was applied. The reflections 002, 21$\bar{3}$, 220, 22$\bar{2}$, 2$\bar{1}$2, and 31$\bar{4}$, exhibiting large negative ΔF values, were later considered to be affected by extinction and were omitted from the least-squares refinement. Atomic scattering factors for all atoms except hydrogen were taken from ref. 8, that of cobalt being corrected for the real part of the anomalous dispersion according to ref. 9, and that of hydrogen was taken from ref. 10.

(*b*) Crystals of (II) [3] were recrystallized from dimethylformamide–toluene. Cell constants were obtained by least-squares refinement of the 2θ values of 36 reflections, accurately centred on a Hilger and Watts four-circle computer-controlled diffractometer.

Intensity data were collected with a ω—2θ scan technique at take-off angle of 3°. All possible independent reflections within 2θ 40° were measured, zirconium-filtered Mo-K_α radiation being used. Data were not collected all at one time: four separate sets were collected, from the same crystal, which had elongated form and dimensions *ca.* 0.80 × 0.20 × 0.20 mm. The crystal was mounted along the longest dimension with *c* axis aligned to coincide with the ϕ axis of the goniostat. There was no significant trend in the intensities of the 3 standard reflections monitored during data collection and deviations were < |4%|. During later refinement scale factors for the four groups of data were separately refined. Their final values closely agree with those calculated from the standard reflections monitored at data collection time. After correction for background, the standard deviation $\sigma(I)$ of the corrected intensity I was estimated [11] and 4 510 reflections having $I \geqslant 2.5\ \sigma(I)$ were considered observed. No correction for absorption was applied, in view of the low value of linear absorption coefficient. Scattering factors used were as for (I).

Structure Determination.—(*a*) The structure of (I) was solved by standard heavy-atom techniques. The positions of bromine and cobalt were obtained from a Patterson synthesis. A series of Fourier syntheses yielded the positions of all the non-hydrogen atoms and showed that one molecule of solvent was present in the asymmetric unit. This was introduced in the final part of the refinement. Least-squares refinement was undertaken with individual isotropic temperature factors and was followed by refinement in the mixed mode, with anisotropic temperature factors for atoms in the co-ordination polyhedron and in the anion. Scale factors were not refined during the latter cycles. The function minimized was $\Sigma w(|F_o| - |F_c|)^2$ and a Hughes-type weighting scheme was adopted, with $w = 1$ for $F_o \leqslant 28$ and $\sqrt{w} = 28/F_o$ for $F_o > 28$. A difference-Fourier calculated at R 0.12 with reflections having $\sin\theta/\lambda \leqslant 0.40$ (*ca.* 65% of the total reflections) gave the positions of 32 (of the total 48) hydrogen atoms, with mean C–H 1.10 Å, and showed that one of the atoms in the solvent molecule was probably equally distributed, between two positions, in a disordered fashion. Separate refinement of the solvent, assigning 0.5 occupancy factor to the disordered atom, did not appreciably improve distances within the ethanol molecule and yielded very high temperature factors. Parameters from this refinement were used for the solvent molecule, without further change, in subsequent structure-factor calculations. Although there are indications from values of the temperature factors that the disordered atom is oxygen, the scattering factor of carbon was used for all atoms in the solvent. Hydrogen atoms in the experimental or calculated (C–H 1.07 Å) position, with

[6] P. Dapporto and L. Sacconi, *J. Chem. Soc.* (*A*), 1970, 1804.
[7] M. Di Vaira and L. Sacconi, *J.C.S. Dalton*, 1975, 493.
[8] D. T. Cromer and J. T. Waber, *Acta Cryst.*, 1965, **18**, 104.
[9] D. T. Cromer, *Acta Cryst.*, 1965, **18**, 17.
[10] 'International Tables for *X*-Ray Crystallography,' vol. III, Kynoch Press, Birmingham, 1962, p. 202.
[11] R. J. Doedens and J. A. Ibers, *Inorg. Chem.*, 1967, **6**, 204.

TABLE 1

[Co(np)Br][PF_6] Positional parameters ($\times 10^4$) and anisotropic * temperature factors ($\times 10^3$), with estimated standard deviations in parentheses

Atom	x/a	y/b	z/c	U_{11}	U_{22}	U_{33}	U_{12}	U_{13}	U_{23}
Br	1 856(3)	535(2)	3 087(2)	99(2)	47(1)	92(2)	−1(1)	22(2)	24(1)
Co	2 688(3)	1 929(2)	3 694(2)	51(3)	43(2)	47(2)	13(2)	13(2)	18(2)
P(1)	3 186(5)	2 400(3)	5 638(4)	40(4)	41(3)	50(3)	9(3)	12(3)	22(2)
P(2)	1 089(5)	2 599(3)	3 171(4)	51(5)	40(3)	43(3)	7(3)	5(3)	15(2)
P(3)	4 515(5)	1 946(3)	2 775(4)	48(4)	40(3)	40(3)	13(3)	10(3)	13(2)
P(4)	2 080(11)	5 476(4)	7 875(6)	104(9)	70(4)	87(5)	45(4)	46(5)	32(4)
F(1)	3 577(23)	5 413(14)	7 866(21)	130(20)	208(25)	262(26)	57(16)	−9(16)	102(20)
F(2)	619(22)	5 525(10)	7 750(19)	126(19)	110(13)	265(25)	44(12)	70(16)	92(15)
F(3)	2 227(31)	5 954(12)	9 084(15)	442(38)	153(17)	103(13)	146(22)	115(20)	62(12)
F(4)	2 352(15)	6 267(8)	7 670(13)	152(14)	66(8)	143(13)	8(8)	49(11)	48(9)
F(5)	1 947(20)	4 995(11)	6 618(13)	232(21)	147(16)	83(11)	76(15)	32(12)	21(10)
F(6)	1 862(23)	4 672(10)	8 083(17)	320(27)	83(11)	209(20)	79(15)	140(20)	90(13)
N	3 908(13)	3 503(7)	4 355(11)	21(10)	36(8)	49(8)	3(6)	9(7)	17(6)

* In the form: $\exp[-2\pi^2(U_{11}h^2a^{*2} + U_{22}k^2b^{*2} + U_{33}l^2c^{*2} + 2U_{12}hka^*b^* + 2U_{13}hla^*c^* + 2U_{23}klb^*c^*)]$.

exclusion of those of the solvent molecule, were introduced in the final set of least-squares cycles. Each was assigned a temperature factor close to that of its own carbon atom.

TABLE 2

[Co(np)Br][PF_6] Positional parameters ($\times 10^3$) and isotropic temperature factors ($\times 10^3$), with estimated standard deviations in parentheses

Atom	x/a	y/b	z/c	U/Å^2
C(1)	441(2)	381(1)	556(2)	48(5)
C(2)	346(2)	350(1)	616(1)	43(5)
C(3)	291(2)	397(1)	415(1)	41(4)
C(4)	197(2)	350(1)	307(2)	48(5)
C(5)	498(2)	358(1)	377(1)	44(5)
C(6)	569(2)	286(1)	354(1)	42(4)
C(7)	458(2)	210(1)	615(2)	55(5)
C(8)	477(3)	133(2)	557(2)	112(9)
C(9)	586(3)	104(2)	603(3)	129(11)
C(10)	652(3)	149(2)	694(3)	118(10)
C(11)	648(3)	228(2)	754(3)	104(9)
C(12)	543(3)	258(2)	711(2)	94(8)
C(13)	195(2)	210(1)	638(2)	52(5)
C(14)	151(2)	130(2)	606(2)	64(6)
C(15)	57(2)	102(2)	662(2)	86(7)
C(16)	16(2)	156(2)	747(2)	77(7)
C(17)	59(3)	238(2)	782(2)	101(9)
C(18)	153(2)	265(1)	745(2)	63(6)
C(19)	7(2)	292(1)	419(2)	55(6)
C(20)	−37(3)	241(1)	475(2)	84(7)
C(21)	−126(3)	264(2)	555(2)	95(8)
C(22)	−158(3)	335(2)	581(2)	97(8)
C(23)	−120(3)	384(2)	530(3)	112(10)
C(24)	−43(2)	364(2)	442(2)	76(7)
C(25)	0(2)	209(1)	187(2)	53(5)
C(26)	−46(2)	253(1)	128(2)	68(6)
C(27)	−132(2)	211(2)	31(2)	76(7)
C(28)	−178(3)	131(2)	−4(2)	93(8)
C(29)	−135(3)	88(2)	56(2)	98(8)
C(30)	−50(2)	130(2)	156(2)	81(7)
C(31)	408(2)	199(1)	141(2)	50(5)
C(32)	281(2)	167(1)	90(2)	57(6)
C(33)	241(3)	172(3)	−13(2)	101(9)
C(34)	337(2)	212(1)	−51(2)	76(7)
C(35)	459(3)	245(2)	−5(2)	101(9)
C(36)	503(2)	240(1)	101(2)	70(6)
C(37)	542(2)	115(1)	257(2)	44(5)
C(38)	496(2)	44(2)	169(2)	76(7)
C(39)	563(3)	−22(2)	159(3)	109(9)
C(40)	670(3)	−17(2)	234(2)	99(8)
C(41)	715(3)	53(2)	319(3)	119(10)
C(42)	648(3)	122(2)	329(2)	99(8)
C(43) *	315(4)	527(3)	239(4)	155(20)
C(44) *	274(8)	503(5)	139(9)	268(41)
C(45,1) *†	147(8)	523(5)	114(6)	138(40)
C(45,2) *†	204(8)	428(5)	67(7)	137(37)

* These atoms belong to the solvent molecule. † Assigned 0.5 population parameter.

The refinement was considered terminated when the mean shift-to-error ratio reached 0.09. The final R is 0.098.

Final values of the parameters and their estimated standard deviations are reported in Tables 1—3. Standard deviations on values of the parameters were calculated by the least-squares program, according to the expression $\sigma_j = [\Sigma\Delta F^2\ a^{jj}/(m-n)]^{1/2}$, where m is the number of reflections, n the number of parameters, and a^{jj} is the jj^{th} element of the inverse least-squares matrix. The factorization of the least-squares matrix due to the separate isotropic and anisotropic refinements performed on different groups of atoms was accounted for by multiplying the σ_j values by suitable factors. Crystallographic calculations

TABLE 3

[Co(np)Br][PF_6] Positional parameters ($\times 10^3$) for hydrogen atoms*

Atom	x/a	y/b	z/c
H(1,1)	532	363	546
H(1,2)	450	442	590
H(2,1)	398	360	703
H(2,2)	215	365	610
H(3,1)	213	396	468
H(3,2)	350	436	420
H(4,1)	128	381	294
H(4,2)	250	335	240
H(5,1)	590	414	412
H(5,2)	460	350	296
H(6,1)	592	287	440
H(6,2)	630	295	320
H(8)	400	90	460
H(9)	620	65	520
H(11)	698	285	830
H(12)	500	315	745
H(14)	171	86	549
H(17)	80	274	848
H(18)	190	345	750
H(20)	−22	182	449
H(22)	−220	350	640
H(23)	−140	430	520
H(24)	10	415	400
H(26)	0	310	160
H(27)	−110	248	−20
H(29)	−138	16	30
H(32)	222	145	132
H(33)	152	121	−50
H(34)	340	212	−150
H(35)	532	270	−30
H(36)	623	255	125
H(38)	420	38	90

* Numbered according to the carbon atom to which they are attached. Co-ordinates of the ten hydrogen atoms introduced in calculated position (see text) are not included here.

were performed on a CII 10070 computer, with the '*X*-Ray '72' set of programs.[12] The program ORTEP [13] was used for drawings of molecular structures and the analysis of the thermal ellipsoids was performed with a local program.

(*b*) The approximate positions of the iodine, cobalt, and phosphorus atoms in (II) were determined from a Patterson synthesis. The non-hydrogen atoms in the cation and in the anion were located with a series of Fourier syntheses. Few cycles of isotropic refinement, followed by mixed refinement during which atoms in the co-ordination polyhedron were assigned anisotropic temperature factors and were separately refined, reduced R to 0.13. A difference-Fourier calculated at this point showed the positions of all carbon atoms of the solvent molecule in the asymmetric unit. These were refined isotropically and their parameters were used without further change in the subsequent F_c calculations. Hydrogen atoms were also introduced, in calculated positions, with B 5.0 Å^2 and not refined. The threshold value for the Hughes-type weighting scheme in the least-squares calculations was F_o 35. After a few cycles in the mixed mode the conventional R halted at 0.115. Two facts were evident at this point: (i) the temperature factor of iodine was abnormally high, being about three times larger than those of the other atoms in the co-ordination polyhedron. There was supporting evidence from the Patterson synthesis for large thermal motion or partial disorder affecting the iodine-atom position. In fact, all vectors involving iodine in the map had peak heights lower than the expected by a factor *ca.* 0.5. (ii) Several low-order reflections showed large positive ΔF values, many having F_c values close to zero. This could be due to an inadequate treatment of the situation at the iodine or solvent positions, or to some other fault in the model.

In an attempt to improve the description, the occupancy factors of atoms in the co-ordination polyhedron were refined, all other parameters being constrained to fixed values. Isotropic temperature factors, identical for all atoms in the polyhedron, were assigned during this refinement. The occupancy factors of atoms other than iodine turned out to be quite close to each other, and that of iodine was lower than their mean by a factor 0.67. After assigning this value to iodine and unit value to all other atoms, refinement was continued on parameters different from the occupancy factors, following the procedure outlined. R Was reduced to 0.088 and the ΔF values of low-order reflections were drastically reduced. The most significant change consisted in a (*ca.* 40%) decrease of the temperature factor of iodine, which, however, was still very high; the atomic positions were essentially unaffected. These results might indicate that the iodine atom is affected by disorder, or even that a halogen atom lighter than iodine is actually co-ordinating. A ΔF Fourier calculated at R 0.088 showed diffuse positive density around the iodine centre, but gave no indication of disorder; it also failed to reveal significant features in the other parts of the asymmetric unit. The hypothesis that the monatomic ligand is not iodine seems unlikely, in view of the elemental analysis and density data. Nevertheless, a few cycles of refinement were attempted using the bromine, rather than the iodine scattering factor, and unit population parameters. No improvement was achieved: R converged to 0.091 and the temperature factor of the halogen was still high, being essentially identical to that attained by iodine with 0.67 population parameter. In conclusion, the iodine atom, present in the structure, is affected by unusually large thermal motion, but it is not in a disordered position. The situation for the halogen atom is similar, to some extent, in the structure of (I) (see later).

TABLE 4

[Co(np)I][BPh_4] Positional parameters ($\times 10^4$) and anisotropic* temperature factors ($\times 10^3$), with estimated standard deviations in parentheses

Atom	x/a	y/b	z/c	U_{11}	U_{22}	U_{33}	U_{12}	U_{13}	U_{23}
I	2 004(1)	856(1)	3 002(2)	112(1)	74(1)	101(1)	1(1)	0(1)	1(1)
Co	1 759(1)	2 043(1)	1 934(2)	28(1)	27(1)	29(1)	3(1)	−3(1)	−9(1)
P(1)	334(2)	2 075(2)	1 777(3)	31(2)	24(2)	30(2)	5(2)	−3(2)	0(2)
P(2)	2 502(2)	2 129(2)	−99(3)	32(2)	29(2)	27(2)	8(2)	−6(2)	−5(2)
P(3)	2 314(2)	2 872(2)	3 341(4)	34(2)	24(2)	32(2)	3(2)	−4(2)	−8(2)
N	1 559(6)	3 368(5)	733(10)	36(7)	29(6)	31(6)	6(5)	−2(5)	3(5)

* See footnote to Table 1.

Although refinement of the occupancy factor of iodine helped to clarify the situation, it was not a completely satisfactory refinement procedure. Since the atomic positions are essentially unaffected by the detailed consideration made for iodine, results obtained at R 0.115, in the first part of the refinement, are reported here as the final results. Values of the positional and thermal parameters appear in Tables 4 and 5.*

Molecular Orbital Calculations.—The well known EH SCCC scheme of calculation was adopted.[14] The diagonal elements (H_{ii}) of the Hamiltonian matrix were assumed equal to the negative of the valence-orbital ionization potentials (VOIP) calculated by Gray *et al.*[15] The off-diagonal elements were calculated according to the Cusachs approximation [16] and were corrected for overlap.[17] There was full consideration of the overlap. Richardson's functions [18] were used for the metal orbitals and Clementi's functions [19] for the orbitals of the other atoms. The secular

* Observed and calculated structure factors for both structures are listed in Supplementary Publication No. SUP 21341 (15 pp., 1 microfiche). See Notice to Authors No. 7 in *J.C.S. Dalton*, 1974, Index issue.

[12] '*X*-Ray '72,' Technical Report TR 192, University of Maryland, 1972, eds. J. M. Stewart, F. A. Kundell, and J. C. Baldwin.

[13] C. K. Johnson, Report ORNL 3794, Oak Ridge National Laboratory, Oak Ridge, Tennessee, 1965.

[14] H. Basch, A. Viste, and H. B. Gray, *J. Chem. Phys.*, 1966, **44**, 10, and refs. therein.

[15] H. Basch, A. Viste, and H. B. Gray, *Theor. Chim. Acta*, 1965, **3**, 458.

[16] L. C. Cusachs and B. B. Cusachs, *J. Phys. Chem.*, 1967, **71**, 1060.

[17] C. J. Ballhausen and H. B. Gray, 'Molecular Orbital Theory,' Benjamin, New York, 1965, p. 118.

[18] J. W. Richardson, W. C. Nieuwpoort, R. R. Powell, and W. F. Edgell, *J. Chem. Phys.*, 1962, **36**, 1057; J. W. Richardson, R. R. Powell, and W. C. Nieuwpoort, *ibid.*, 1963, **38**, 796.

[19] E. Clementi, 'Tables of Atomic Functions,' IBM Corp., San Jose, California, 1965.

TABLE 5

[Co(np)I][BPh_4] Positional parameters ($\times 10^3$) and isotropic temperature factors ($\times 10^3$), with estimated standard deviations in parentheses

Atom	x/a	y/b	z/c	U/Å²
C(1)	70(1)	338(1)	38(1)	41(4)
C(2)	12(1)	302(1)	149(1)	39(4)
C(3)	208(1)	351(1)	−50(2)	37(4)
C(4)	211(1)	281(1)	−122(2)	41(4)
C(5)	178(1)	392(1)	163(2)	42(4)
C(6)	251(1)	374(1)	241(1)	40(4)
C(7)	−35(1)	169(1)	313(1)	31(4)
C(8)	−95(1)	205(1)	363(2)	56(5)
C(9)	−149(1)	173(1)	464(2)	71(5)
C(10)	−141(1)	103(1)	511(2)	68(5)
C(11)	−83(1)	66(1)	464(2)	56(5)
C(12)	−29(1)	99(1)	364(2)	51(4)
C(13)	−7(1)	164(1)	39(1)	33(4)
C(14)	−81(1)	178(1)	−4(2)	79(6)
C(15)	−141(2)	133(1)	−107(3)	102(7)
C(16)	−71(1)	85(1)	−148(2)	88(7)
C(17)	−1(1)	71(1)	−111(2)	69(5)
C(18)	33(1)	113(1)	−10(2)	54(4)
C(19)	249(1)	134(1)	−101(2)	33(3)
C(20)	209(1)	127(1)	−213(2)	54(4)
C(21)	206(1)	64(1)	−274(2)	72(5)
C(22)	238(2)	4(1)	−225(2)	90(7)
C(23)	279(1)	11(1)	−104(2)	93(7)
C(24)	286(1)	77(1)	−47(2)	76(6)
C(25)	358(1)	242(1)	4(1)	37(4)
C(26)	396(1)	216(1)	114(2)	63(5)
C(27)	480(1)	240(1)	124(2)	73(5)
C(28)	520(1)	280(1)	31(2)	86(6)
C(29)	486(2)	307(1)	−79(2)	89(6)
C(30)	399(1)	286(1)	−90(2)	74(6)
C(31)	324(1)	271(1)	421(1)	37(4)
C(32)	392(1)	319(1)	399(2)	59(5)
C(33)	462(1)	302(1)	473(2)	83(6)
C(34)	459(1)	244(1)	561(2)	75(6)
C(35)	390(1)	197(1)	580(2)	84(6)
C(36)	322(1)	213(1)	507(2)	61(5)
C(37)	158(1)	299(1)	465(1)	33(3)
C(38)	153(1)	367(1)	519(2)	45(4)
C(39)	94(1)	369(1)	617(2)	62(5)
C(40)	44(1)	312(1)	661(2)	63(5)
C(41)	47(1)	248(1)	616(2)	61(5)
C(42)	105(1)	239(1)	516(2)	51(4)
C(43)	−250(1)	412(1)	−8(1)	35(4)
C(44)	−313(1)	439(1)	−82(2)	52(4)
C(45)	−311(1)	440(1)	−218(2)	58(4)
C(46)	−252(1)	419(1)	−285(2)	69(5)
C(47)	−186(1)	393(1)	−219(2)	68(5)
C(48)	−188(1)	390(1)	−81(2)	44(4)
C(49)	−283(1)	317(1)	206(1)	36(4)
C(50)	−321(1)	297(1)	330(2)	60(5)
C(51)	−347(1)	225(1)	376(2)	74(6)
C(52)	−334(1)	170(1)	290(2)	79(6)
C(53)	−297(1)	188(1)	166(2)	78(6)
C(54)	−273(1)	261(1)	128(2)	49(4)
C(55)	−162(1)	421(1)	213(1)	27(3)
C(56)	−143(1)	398(1)	338(2)	42(4)
C(57)	−68(1)	418(1)	392(2)	48(4)
C(58)	−10(1)	463(1)	320(2)	43(4)
C(59)	−27(1)	489(1)	198(1)	35(3)
C(60)	−102(1)	467(1)	146(1)	35(3)
C(61)	−316(1)	453(1)	219(1)	34(3)
C(62)	−292(1)	511(1)	290(2)	46(4)
C(63)	−348(1)	553(1)	344(2)	60(5)
C(64)	−428(1)	537(1)	329(2)	68(5)
C(65)	−455(1)	480(1)	263(2)	62(5)
C(66)	−401(1)	440(1)	210(2)	52(4)
C(67) *	573(2)	14(2)	703(4)	177(8)
C(68) *	523(2)	38(2)	800(4)	203(10)
C(69) *	542(2)	102(2)	877(5)	164(9)
C(70) *	602(2)	141(2)	835(4)	215(10)
C(71) *	649(2)	129(2)	748(4)	190(9)
C(72) *	633(2)	67(2)	678(4)	152(8)
C(73) *	561(2)	−39(2)	628(4)	190(9)
B	−252(1)	402(1)	157(2)	35(4)

* These atoms belong to the solvent molecule.

equation was solved by the Löwdin symmetric orthogonalization procedure [20] and a Löwdin population analysis [20] was performed. The test value for self-consistency was 0.001 on all parameters. For group overlap calculations a program originally written by Prof. L. Oleari of the Istituto di Chimica Fisica in Parma for two-centre overlaps and locally modified was used. For calculations of molecular geometries, for the self-consistent calculations, and for population analysis I used my own programs for the IBM 1130.

The geometry of the model cations investigated is schematized in Figure 1. Models will be denoted M(L)X, where M = Co or Ni, X = Cl or Br (iodine could not be considered for lack of orbital functions and VOIP values

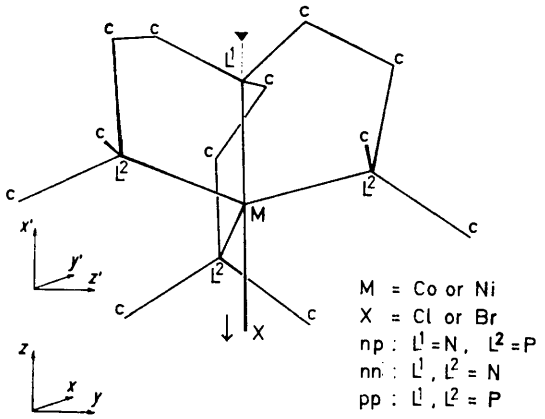

FIGURE 1 The molecular models used in the calculations. Local right-handed cartesian axes are: (a) x, y, z, with $z \parallel 3$ (3 = three-fold axis) for centres M, X, and L^1; (b) x', y', z', with $x' \parallel 3$ and $z' \perp 3$ for the L^2 and c centres. Arrow indicates positive sense in the shift of the M–X group distortion. M = Co or Ni, X = Cl or Br; np : L^1 = N, L^2 = P; nn : L^1 = L^2 = N; pp : L^1 = L^2 = P

homogeneous with those used for the other atoms) and L is the terdentate tripod ligand: np = tris(2-diphenylphosphinoethyl)amine, nn = tris(2-dimethylaminoethyl)amine, or pp = tris(2-diphenylphosphinoethyl)phosphine.

The experimental geometries from refs. 4, 7, and 21—23 were referred to and idealized, where necessary, to C_3 symmetry. The high-[4] and low-spin [7] geometries of np complexes are reproduced by models denoted [M(np)X] (A) and [M(np)X] (B), respectively. Approximations had to be imposed, in order to reduce the size of calculations: each phenyl group was substituted by one carbon atom (Figure 1), hydrogen atoms were ignored, and all 'carbon' centres in Figure 1 were treated as one-electron atoms, each being assigned one 2*s* orbital, to simulate the overlap by spherical shells. The 2*p* rather than the 2*s* VOIP function was used for these, however, because *ca.* 70% of the charge residing in the valence shell of carbon atoms belongs to 2*p* orbitals. Ligand atoms were assigned all their valence-shell *s* and *p* orbitals and for the metal atom the 3*d*, 4*s*, and 4*p* sets were used.

With each of the above simplified geometries all combinations of metal (Co or Ni) and halogen (Cl or Br) atoms and both spin states were investigated. Although some models

[20] P. O. Löwdin, *J. Chem. Phys.*, 1950, **18**, 365.
[21] M. Di Vaira and P. L. Orioli, *Inorg. Chem.*, 1967, **6**, 955.
[22] M. Di Vaira and P. L. Orioli, *Acta Cryst.*, 1968, **B24**, 595.
[23] M. Di Vaira and L. Sacconi, *Abs. 6th Natl. Meeting Ital. Assocn. Inorg. Chem.*, 1973, B5; also data to be published.

would thus correspond to complete idealizations useful comparisons were expected with the other 'real' cases. Only results considered to be of interest will be discussed here. The effects of the tetrahedral distortion were investigated by shifting the M–X group along the three-fold axis as shown in Figure 1.

DISCUSSION

Description of the Structures.—(a) The structure of the bromine derivative (I) consists of $[Co(np)Br]^+$ cations, $[PF_6]^-$ anions, and of intermixed ethanol molecules, occupying partly disordered positions. The cation is shown in Figure 2. Selected values of bond distances and angles are reported in Table 6.

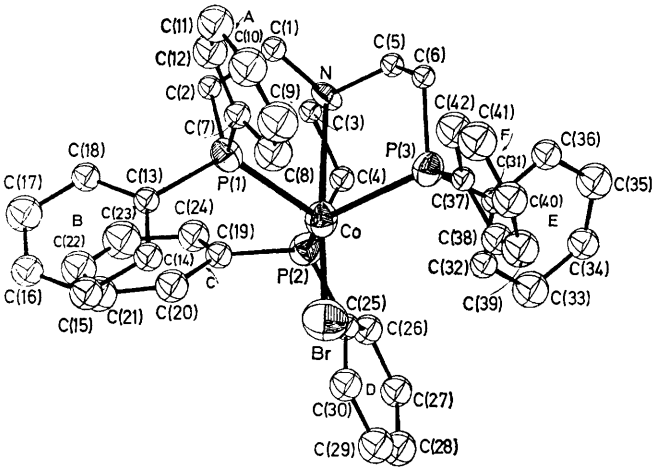

FIGURE 2 Perspective view of the cation $[Co(np)Br]^+$, showing the atom labelling. 50% Probability contours for the ellipsoids of atoms in the co-ordination polyhedron are shown, and 25% contours for other atoms

The co-ordination about the metal is trigonal bipyramidal, with a large tetrahedral distortion of the sort found in the corresponding chloro-derivative, (III).[4] The distortion in (I) is larger than in (III), the Co–N distance being 2.73(1) Å and the mean Br–Co–P angles 106.0° [corresponding values in (III), 2.67(1) Å and 104.6°]. The metal atom lies 0.65 Å [0.60 Å in (III)] below the plane of the phosphorus atoms. The mean Co–P distance (2.37 Å) matches that (2.37 Å) in (III) and the short Co–Br distance [2.357(4) Å] exceeds Co–Cl in (III) by 0.13 Å, which is slightly less than the difference between the covalent radii of the two halogens.[24]

The temperature factor of the bromine is quite large, although it is not as large as that of iodine in complex (II). Evidently, there is a connection between these features of the two structures (see later). Bond angles at phosphorus in the cation (Table 6) agree with those in (III), and the importance of the equatorial phosphorus donors to the tetrahedral distortion established for (III)[4] also apply to the present case. The absence of strains in the chains of the ligand (Table 6) indicates[4] that the geometry of the ligand molecule is compatible with tetrahedral elongations in the co-ordination, even larger than for (III). The similarity of co-ordination geometry in the structures of (I) and (III) indicates that forces due to packing in the solid do not determine the tetrahedral distortion in these cobalt complexes [with the possible exception of (II)]. The mean P–F distance (1.55 Å uncorrected) in the anion is identical to that in

TABLE 6

$[Co(np)Br][PF_6]$ Interatomic distances (Å) and angles (°), with standard deviations in parentheses

(*a*) Bond lengths

Co–Br	2.357(4)	P(2)–C(25)	1.81(2)
Co–P(1)	2.361(6)	P(3)–C(6)	1.81(2)
Co–P(2)	2.402(7)	P(3)–C(31)	1.84(2)
Co–P(3)	2.355(7)	P(3)–C(37)	1.80(2)
Co–N	2.731(12)	N–C(1)	1.49(3)
		N–C(3)	1.51(3)
P(1)–C(2)	1.83(2)	N–C(5)	1.43(3)
P(1)–C(7)	1.80(2)	C(1)–C(2)	1.49(3)
P(1)–C(13)	1.81(2)	C(3)–C(4)	1.53(2)
P(2)–C(4)	1.80(2)	C(5)–C(6)	1.55(3)
P(2)–C(19)	1.78(2)		

(*b*) Bond angles

Br–Co–P(1)	106.4(0.2)	C(4)–P(2)–C(25)	105.2(1.0)
Br–Co–P(2)	110.3(0.2)	C(19)–P(2)–C(25)	105.7(1.0)
Br–Co–P(3)	101.3(0.2)	Co–P(3)–C(6)	109.0(0.6)
Br–Co–N	173.8(0.4)	Co–P(3)–C(31)	111.1(0.7)
P(1)–Co–P(2)	110.2(0.2)	Co–P(3)–C(37)	118.6(0.7)
P(1)–Co–P(3)	114.6(0.2)	C(6)–P(3)–C(31)	105.4(0.9)
P(2)–Co–P(3)	113.4(0.3)	C(6)–P(3)–C(37)	104.9(0.9)
P(1)–Co–N	74.2(0.3)	C(31)–P(3)–C(37)	106.8(0.9)
P(2)–Co–N	74.8(0.3)	Co–N–C(1)	109.0(1.1)
P(3)–Co–N	73.1(0.3)	Co–N–C(3)	107.6(0.8)
		Co–N–C(5)	110.9(0.9)
Co–P(1)–C(2)	107.4(0.7)	C(1)–N–C(3)	109.4(1.2)
Co–P(1)–C(7)	115.1(0.7)	C(1)–N–C(5)	108.9(1.3)
Co–P(1)–C(13)	117.6(0.6)	C(3)–N–C(5)	111.1(1.5)
C(2)–P(1)–C(7)	109.1(0.8)	N–C(1)–C(2)	110.9(1.3)
C(2)–P(1)–C(13)	105.1(0.9)	P(1)–C(2)–C(1)	109.8(1.2)
C(7)–P(1)–C(13)	101.9(1.1)	N–C(3)–C(4)	112.1(1.3)
Co–P(2)–C(4)	106.7(0.7)	P(2)–C(4)–C(3)	108.7(1.4)
Co–P(2)–C(19)	112.5(0.8)	N–C(5)–C(6)	112.3(1.6)
Co–P(2)–C(25)	119.5(0.8)	P(3)–C(6)–C(5)	107.8(1.2)
C(4)–P(2)–C(19)	106.2(0.9)		

(*c*) Phenyl rings

	Mean	Mean devn.	Max. devn.
(i) Bond lengths			
Ring			
A	1.39	0.06	0.15
B	1.38	0.02	0.04
C	1.39	0.05	0.09
D	1.38	0.01	0.02
E	1.39	0.03	0.07
F	1.40	0.05	0.10
(ii) Bond angles			
Ring			
A	119.9	2.9	7.8
B	118.9	1.6	3.3
C	119.9	1.9	3.0
D	119.9	1.1	2.5
E	120.0	4.6	8.6
F	120.0	1.7	3.3

(III); it is slightly larger than that in $[Ni(np)Cl][PF_6]$ (ref. 7), but it is much shorter than in structures where thermal motion is not high.[25] The temperature factors of the fluorine atoms are high, but there is no evidence of disorder. There are no unusually short contacts in the structure. Shortest intermolecular contacts involving fluorine atoms and contact distances <3.60 Å between non-hydrogen atoms are listed in Table 7.

[24] L. Pauling and M. L. Huggins, *Z. Krist.*, 1934, **87**, 205.
[25] H. Bode and G. Teufer, *Z. anorg. Chem.*, 1952, **268**, 20; *Acta Cryst.*, 1955, **8**, 611.

TABLE 7

Short intermolecular contacts (Å) in the structure of [Co(np)Br][PF_6]

F(4) · · · C(36^{I})	3.25	C(22) · · · C(43^{II})	3.51
F(4) · · · C(6^{I})	3.25	C(33) · · · C(40^{III})	3.55
F(4) · · · C(26^{II})	3.19	C(34) · · · C(39^{III})	3.58
F(2) · · · C(45,1^{II})	3.14	C(34) · · · C(40^{III})	3.29
C(1) · · · C(43^{I})	3.30	C(21) · · · C(42^{IV})	3.54

Superscripts refer to the following equivalent positions relative to the reference molecule at x, y, z:

I $1-x, 1-y, 1-z$ III $1-x, -y, -z$
II $-x, 1-y, 1-z$ IV $x-1, y, z$

(*b*) The structure of the iodo-derivative (II) consists of $[Co(np)I]^+$ cations, tetraphenylborate anions, and toluene molecules from the solvent. The two ions, with the labelling of the atoms, are shown in Figure 3. The

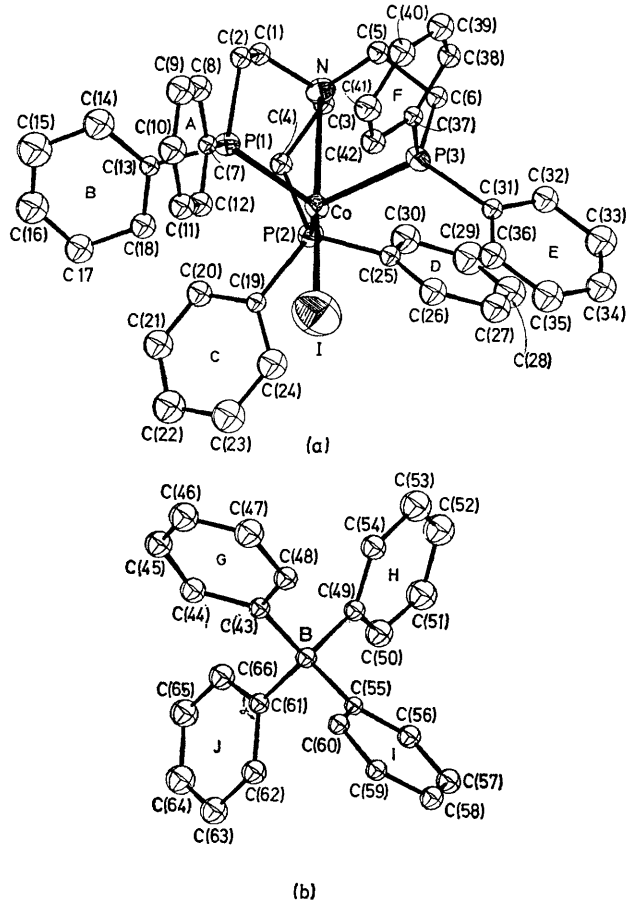

FIGURE 3 Perspective view of (a) the cation and (b) the anion of [Co(np)I][BPh_4]. Contours are as for Figure 2

co-ordination about the metal is similar to that in complexes (I) and (III). Since this is the only high-spin iodo-derivative of cobalt in this series, determination of its structure establishes that the 4 + 1 intermediate co-ordination is necessarily associated with the high-spin state of the metal. Similar co-ordination geometry has recently been found for other high-spin cobalt(II) complexes with tripod ligands containing mixed-donor sets different from that of np.[2b] The geometry of the $[Co(np)I]^+$ chromophore in the low-spin state [5] is fundamentally different from that in (II) and no conclusive comparisons can be drawn between the present complex and the complex [Co(np)I]I (ref. 5). Selected bond distances and angles are reported in Table 8.

TABLE 8

[Co(np)I][BPh_4] Interatomic distances (Å) and angles (°), with standard deviations in parentheses

(*a*) Bond lengths

Co–I	2.466(2)	P(2)–C(25)	1.83(2)
Co–P(1)	2.375(4)	P(3)–C(6)	1.81(2)
Co–P(2)	2.355(4)	P(2)–C(31)	1.83(2)
Co–P(3)	2.351(4)	P(3)–C(37)	1.81(2)
Co–N	2.725(10)	N–C(1)	1.48(2)
		N–C(3)	1.49(2)
P(1)–C(2)	1.84(2)	N–C(5)	1.47(2)
P(1)–C(7)	1.81(2)	C(1)–C(2)	1.52(2)
P(1)–C(13)	1.81(2)	C(3)–C(4)	1.55(2)
P(2)–C(4)	1.82(2)	C(5)–C(6)	1.52(2)
P(2)–C(19)	1.82(2)		

(*b*) Bond angles

I–Co–P(1)	108.1(0.1)	C(4)–P(2)–C(25)	105.9(0.7)
I–Co–P(2)	104.0(0.1)	C(19)–P(2)–C(25)	104.6(0.7)
I–Co–P(3)	104.9(0.1)	Co–P(3)–C(6)	108.7(0.5)
I–Co–N	177.5(0.4)	Co–P(3)–C(31)	120.8(0.5)
P(1)–Co–P(2)	115.3(0.2)	Co–P(3)–C(37)	110.5(0.5)
P(1)–Co–P(3)	111.9(0.2)	C(6)–P(3)–C(31)	106.2(0.7)
P(2)–Co–P(3)	111.7(0.2)	C(6)–P(3)–C(37)	105.9(0.7)
P(1)–Co–N	74.4(0.2)	C(31)–P(3)–C(37)	103.8(0.7)
P(2)–Co–N	74.4(0.3)	Co–N–C(1)	108.6(0.7)
P(3)–Co–N	74.2(0.3)	Co–N–C(3)	109.8(0.8)
		Co–N–C(5)	109.8(0.8)
Co–P(1)–C(2)	108.6(0.5)	C(1)–N–C(3)	108.4(1.0)
Co–P(1)–C(7)	120.5(0.5)	C(1)–N–C(5)	110.2(1.1)
Co–P(1)–C(13)	113.3(0.5)	C(3)–N–C(5)	110.0(1.0)
C(2)–P(1)–C(7)	105.3(0.7)	N–C(1)–C(2)	111.9(1.1)
C(2)–P(1)–C(13)	105.5(0.7)	P(1)–C(2)–C(1)	108.1(1.0)
C(7)–P(1)–C(13)	102.4(0.6)	N–C(3)–C(4)	111.0(1.0)
Co–P(2)–C(4)	108.5(0.5)	P(2)–C(4)–C(3)	108.6(1.0)
Co–P(2)–C(19)	118.5(0.5)	N–C(5)–C(6)	111.1(1.2)
Co–P(2)–C(25)	113.2(0.5)	P(3)–C(6)–C(5)	110.3(1.0)
C(4)–P(2)–C(19)	105.2(0.7)		

(*c*) Phenyl rings

	Mean	Mean devn.	Max. devn.
(i) Bond lengths			
Ring			
A	1.38	0.02	0.03
B	1.37	0.08	0.12
C	1.38	0.02	0.05
D	1.37	0.06	0.11
E	1.38	0.03	0.05
F	1.38	0.04	0.07
G	1.37	0.04	0.11
H	1.40	0.01	0.03
I	1.38	0.01	0.03
J	1.38	0.02	0.04
(ii) Bond angles *			
Ring			
A	120.0	1.1	2.0
B	120.0	3.4	7.9
C	118.8	2.7	4.6
D	120.0	2.5	6.4
E	120.0	2.0	3.6
F	120.0	1.2	2.9
G	120.0		
H	120.0		
I	120.0		
J	120.1		

* Angles in phenyl rings of the anion are affected by systematic distortions (see text), and deviations from the means are not given here.

The Co–I distance [2.466(2) Å] is shorter than expected from the metal–halogen distances in (I) and (III) and

from the differences between the covalent radii of the halogen atoms.[24] The mean Co–P value (2.36 Å) agrees with those in the other two structures. The Co–N distance [2.72(1) Å] is comparable to that in (I). The mean I–Co–P angle (105.6°) and the distance (0.64 Å) of the metal atom from the plane of the phosphorus atoms, also indicate that the tetrahedral distortion in this complex is comparable to that in (I) [it is possibly slightly lower in (II) than in (I)].

Distances and angles in the ligand molecule are normal.[26] Angles at the carbon atoms bonded to boron in the phenyl rings of the anion (denoted by α in Figure 3), are all smaller than 120°, mean 114.6°. This has been observed previously for tetraphenylborate,[27] and is probably indicative of some hindrance between the substituents at boron. Therefore in addition to being bulky, the anion is not very flexible. It may thus provide a suitable matrix to stabilize the high-spin state and geometry of the cation through packing in the solid. There are few short intermolecular contacts in the structure. Those <3.60 Å are listed in Table 9.

TABLE 9

Intermolecular contacts <3.60 Å in the structure of [Co(np)I][BPh_4]

C(3) · · · C(62^{I})	3.54	C(17) · · · C(18^{II})	3.55
C(6) · · · C(45^{I})	3.53	C(20) · · · C(36^{III})	3.53
C(17) · · · C(17^{II})	3.33		

Superscripts refer to the following equivalent positions relative to the reference molecule at x, y, z:

I $-x, 1-y, -z$ III $x, y, z-1$
II $-, x-y, -z$

Thermal Vibrations of the Halogen Atoms.—The high temperature factors of the halogen atoms in these structures deserve a comment. The temperature factor [4] of chlorine in (III) was larger than those of the other donor atoms; however, it was still in the normal range. The root-mean-square displacements along the principal axes of the thermal ellipsoids are 0.338, 0.295, and 0.207 Å for bromine and 0.339, 0.324, and 0.266 Å for iodine (standard deviations <0.007 Å). In both cases the two largest axes have comparable magnitude and the lowest one makes a small angle with the direction of the metal–halogen bond [8.7° (I) and 24.5° (II)].

A possible rationalization may be obtained in terms of a pseudo-Jahn–Teller effect,[28] due to interaction between the fundamental $^4A_2$ state (in C_{3v} symmetry) and the excited ^2E, *via* a vibration of proper symmetry. The pseudo-Jahn–Teller effect may cause abnormally low force-constants for some normal modes, or permanent distortions of the geometry, depending on the relative magnitude of some matrix elements in the perturbation expansion.[29] The effect should be appreciable even for values of the energy difference between the two levels involved, much larger than kT,[29] so that magnetic anomalies need not be expected. Being due to second-order perturbation, the effect should increase with decreasing separation between the levels. This is indeed the sense (Cl→I) of increasing stabilization of the low-spin state in this series of complexes, caused by the increasing nephelauxetic effect due to the halogen atom.[25] Detailed consideration shows that, assuming C_{3v} symmetry for the present case, a vibration of Γ_3 symmetry (in double-group notation, corresponding to E in C_{3v}) may connect the fundamental Γ_4 state, originating from the $^4A_2$ under spin–orbit perturbation,[25,30] with the Γ_6 component of ^2E. Although the actual symmetry is lower than C_{3v}, it should be noted that displacements of the E mode are normal to the three-fold axis, in agreement with the orientation of the thermal ellipsoids. This deformation may trace the path toward the low-spin ^{5} conformation.

Results of Molecular Orbital Calculations.—Properties of the ground state of model cations were investigated. Figure 4 shows the ordering of the highest-occupied and of the lowest-unoccupied energy levels, for the high-spin [Co(np)Cl] (A) and the low-spin [Ni(np)Cl] (B) models; the effect on the orbital energies of imposing the tetrahedral distortion is also shown. Similar trends were found for the other models. The orbital pattern agrees with that predicted by the ligand-field approach in the strong-field limit [31] for the d orbitals of the metal. However, participation of the ligand orbitals in the molecular orbitals shown in Figure 4 is significant. As indicated, the contribution of individual metal d orbitals to the e levels varies considerably under the effect of the distortion imposed. The energy of the highest-occupied a (*ca.* z^2) level is strongly affected by the distortion, in particular for the ' expanded ' geometry of the high-spin complexes of the np series [Figure 4(a)]. At very large elongations, this a level and the nearest occupied e level tend to be degenerate, as in tetrahedral co-ordination. However, they are certainly not degenerate at the experimental conformation, as Figure 4 shows; *i.e.* the perturbation due to the apical donor atom in the ligand is significant. The Co–N bond-order varies by *ca.* 50% along the path shown in Figure 4(a).

TABLE 10

Effect of the distortion on d-orbital populations *

		(1)	(2)	(3)
Co	d_{z^2}	1.46	1.42	1.37
	$d_{xy} + d_{x^2-y^2}$	2.80	3.12	3.30
	$d_{xz} + d_{yz}$	3.76	3.38	3.20
Ni	d_{z^2}	1.58	1.55	1.52
	$d_{xy} + d_{x^2-y^2}$	3.50	3.60	3.68
	$d_{xz} + d_{yz}$	3.86	3.72	3.66

* Values of d-orbital populations for cobalt and nickel have been respectively obtained from calculations on the following two high-spin models: [Co(np)Cl] (A) and [Ni(np)Cl] (A). Sums over degenerate orbitals are taken. Values in columns (1) and (3) were calculated for −0.5 and 0.25 Å of the elongation; the positive sense of the distortion is shown in Figure 1. Values in column (2) are for the experimental conformation.

[26] *Chem. Soc. Special Publ.*, No. 18, 1965.
[27] M. Di Vaira and A. Bianchi Orlandini, *J.C.S. Dalton*, 1972, 1704.
[28] W. Öpik and M. H. L. Pryce, *Proc. Roy. Soc.*, 1975, **A238**, 425.
[29] R. G. Pearson, *J. Amer. Chem. Soc.*, 1969, **91**, 4947.
[30] D. Gatteschi and I. Bertini, *Abs. 3rd Natl. Meeting Ital. Assocn. Inorg. Chem.*, 1970, C34.
[31] M. Ciampolini, *Structure and Bonding*, 1969, **6**, 52.

Figure 5 shows the effect of the tetrahedral elongation on the total energy, calculated as the sum of the orbital energies, weighted according to orbital occupancy. The significance of the individual curves is certainly questionable, in view of the approximations proper to the method [32] and of the additional simplifying assumptions made; however comparisons between similar models should be possible. Comparison of the trends in parts

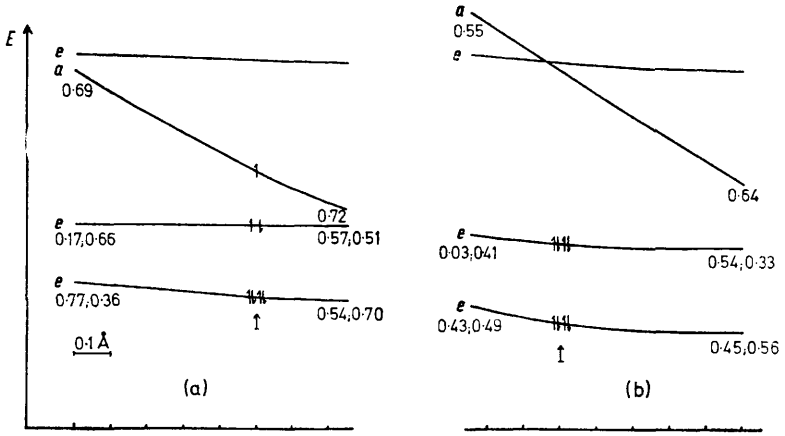

FIGURE 4 The highest-filled and lowest-empty molecular orbitals for (a) high-spin Co(np)Cl (A) and (b) low-spin Ni(np)Cl (B). Ordinates are in arbitrary energy units; tetrahedral distortion increases, along the abscissae, from left to right. Arrows mark the exerimental conformations in refs. 4 and 7 for (a) and (b) respectively. Values of the d_{z^2} eigenvector coefficient are reported for the a level (C_3 symmetry); values for the degenerate levels are geometric means in the order: $(d_{xz}^2 + d_{yz}^2)^{1/2}$, $(d_{xy}^2 + d_{x^2-y^2}^2)^{1/2}$

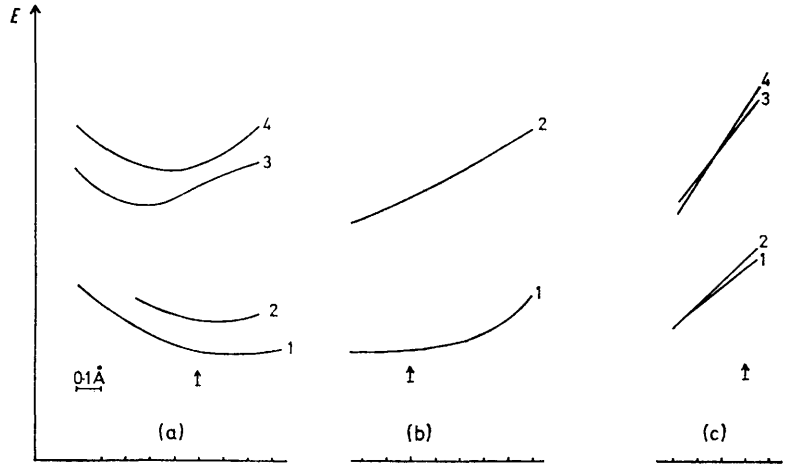

FIGURE 5 Trends in total energy *vs.* elongation. Axes are as in Figure 4. The zero of energy is shifted for separate groups of curves. Curves refer to: (a) 1, Co(np)Cl (A); 2, Co(np)Br (A); 3, Ni(np)Cl (A); and 4, Ni(np)Br (A), all high-spin; (b) 1, Co(np)Cl (B); and 2, Ni(np)Cl (B), both low-spin; (c) 1, high-spin Co(pp)Br; 2, low-spin Co(pp)Br; 3, high-spin Ni(pp)Br; and 4, low-spin Ni(pp)Br. Arrows mark conformations specified in Figure 4, for (*a*) and (*b*), and the conformation having the metal in the plane of the phosphorus atoms [for (*c*)]

(a)—(c) of Figure 5 shows that the tendency toward tetrahedral elongation is largest for the high-spin M(np)X (A) models [Figure 5(a)]. Changing the metal atom affects the energy trends of all M(np)X models [(a) and (b)] and in particular those of the low-spin M(np)X (B) [Figure 5(b)]. On the other hand, when a phosphorus atom occupies the ligand apical position [Figure 5(c)], the energy trends are calculated to be practically independent of the nature of the metal atom models. First, the trend shown by the H_{ii} value of the *d* shell of cobalt closely follows that of the total energy of Co(np)X (A) in Figure 5(a) and seems to be determinant for it. This is not observed for nickel. Secondly, a notable rearrangement of charge within the *d* shell takes place in the course of the distortion (Table 10). The rearrangement is larger for cobalt than for

[32] L. C. Allen, *J. Chem. Phys.*, 1967, **46**, 1029; B. M. Deb and C. A. Coulson, *J. Chem. Soc.* (*A*), 1971, 958.

nickel, probably because the *d* shell of the latter is close to completion. Since shifts in the populations of individual *d* orbitals are dictated by a change in their bonding or antibonding character, a more pronounced stereochemical activity is then expected for cobalt than for nickel, in complexes of this series.

Among the effects due to the specific nature of the donor set, are the following: the M–P overlap reaches a maximum in the proximity of the experimental conformation of [M(np)X] (A) and the M–P bond-order (for the high-spin configuration) is largest at that conformation. Therefore the presence of equatorial phosphorus atoms seems to favour the tetrahedral elongation which is found.

I thank Professor L. Sacconi for suggesting the problem and for his interest in this research.

[4/1647 *Received, 5th August,* 1974]